Leukemia & Lymphoma, January 2006; 47(1): 9–14

Taylor & Francis
Taylor & Francis Group

REVIEW

DNA micro-array analysis of myelodysplastic syndrome

HIROYUKI MANO

Division of Functional Genomics, Jichi Medical School, Kawachigun, Tochigi, Japan

Abstract
Myelodysplastic syndrome (MDS) is an enigmatic disorder characterized by ineffective hematopoiesis and dysplastic morphology of blood cells. The clinical course of MDS consists of distinct stages, with early stages often progressing to advanced ones or to acute myeloid leukemia (AML). Little is known of the molecular pathogenesis of MDS or of the mechanism of its stage progression. DNA micro-array analysis, which allows simultaneous monitoring of the expression levels of tens of thousands of genes, has the potential to provide insight into the pathophysiology of MDS. Several studies have applied this new technology to compare gene expression profiles either between MDS and the healthy condition, among the different stages of MDS or between MDS-derived AML and *de novo* AML. Selection of an appropriate hematopoietic fraction is important for such studies, which to date have been performed with differentiated granulocytes, $CD34^+$ progenitors and $CD133^+$ immature cells. These studies have revealed that each stage of MDS has its own 'molecular signature', indicating the feasibility of differential diagnosis of MDS based on gene expression profile. They have also demonstrated that the current clinical diagnosis of MDS results in the misclassification of patients with regard to these molecular signatures.

Keywords: *Myelodysplastic syndrome, DNA micro-array, acute myeloid leukemia, stage progression, gene expression profile*

Introduction

Myelodysplastic syndrome (MDS) is an enigmatic disorder that is characterized by 2 clinical manifestations: ineffective hematopoiesis (cytopenia in peripheral blood despite hyper- or normal cellularity in bone marrow) and dysplastic morphology of blood cells [1]. MDS mostly affects the elderly, with an incidence of 15–50 cases per 100 000 people per year [2]. Clonality in multiple lineages of blood cells is found in individuals with MDS, suggesting that MDS is a clonal disorder of multi-potent stem cells in bone marrow [3].

An important aspect of MDS is that it comprises different clinical stages. According to the World Health Organization (WHO) classification of MDS [4], affected individuals whose bone marrow contains < 5% blasts are diagnosed with refractory anemia (RA), RA with ringed sideroblasts (RARS), refractory cytopenia with multi-lineage dysplasia (RCMD) or refractory cytopenia with multi-lineage dysplasia and ringed sideroblasts (RCMD-RS), whereas those whose bone marrow contains 5–9% or 10–19% blasts are diagnosed with RA with excess blasts (RAEB)-1 or RAEB-2, respectively. About 10–30% of MDS patients at the early stages (RA, RARS, RCMD or RCMD-RS) will eventually undergo stage progression to RAEB and, subsequently, to acute myeloid leukemia (AML).

Despite the relatively high incidence of MDS, its molecular pathogenesis is poorly understood (Figure 1). Gene mutations or other genomic alterations that might give rise to RA or RCMD remain to be identified and the ineffective hematopoiesis apparent in MDS patients remains to be characterized at the molecular biological level. It is also not known what triggers progression of early stages of MDS to advanced ones in some individuals but not others.

Cytopenia in peripheral blood is also found in patients with aplastic anemia (AA). Although the bone marrow of most individuals with AA is characterized by hypocellularity, the difference in marrow cellularity between patients with AA and those with RA or RCMD is not always clear. Antithymocyte globulin, a standard treatment for AA, is also effective in a sub-set of patients at the early

Correspondence: Hiroyuki Mano, MD, PhD, Division of Functional Genomics, Jichi Medical School, 3311-1 Yakushiji, Kawachigun, Tochigi 329-0498, Japan. Tel: +81-285-58-7449. Fax: +81-285-44-7322. E-mail: hmano@jichi.ac.jp

Received for publication 15 July 2005.

ISSN 1042-8194 print/ISSN 1029-2403 online © 2006 Taylor & Francis
DOI: 10.1080/10428190500264231

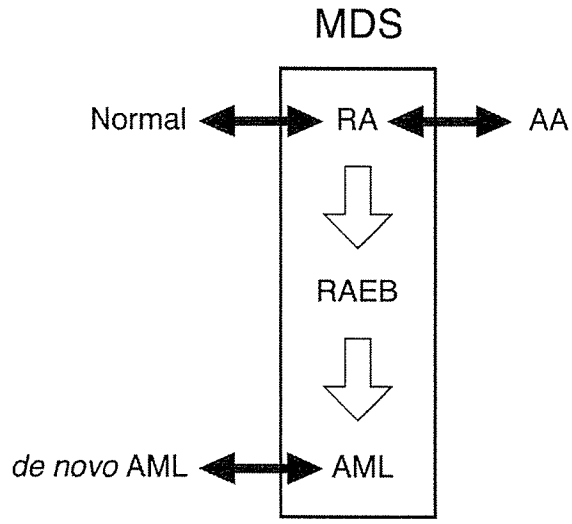

Figure 1. Stage progression of MDS and its relation to other conditions. Little is currently known of the molecular pathogenesis of MDS or of the similarities or differences between the early stages of MDS and aplastic anemia (AA) and between MDS-derived AML and *de novo* AML.

stages of MDS [5], further complicating the distinction between the two disorders.

It is widely believed that AML evolved from MDS has a poorer prognosis than does *de novo* AML, suggesting that the 2 clinical entities might be distinct. However, patients with MDS-associated AML are often older than are those with *de novo* AML and tend to possess karyotypes associated with high risk. It, thus, remains unclear whether the prognosis of *de novo* AML does indeed differ from that of MDS-associated AML if patient age and karyotype are matched.

The Human Genome Project is now close to completion, with 99% of DNA in euchromatin having been sequenced at 99.999% accuracy (http://www.ncbi.nlm.nih.gov/genome/guide/human/). Annotation of the human genome has revealed an unexpectedly small number (20 000 – 25 000) of protein-coding genes [6] compared with the numbers identified in the nematode (~19 000 genes) [7] and fruit fly (~14 000 genes) genomes [8]. The development of DNA micro-array analysis now allows simultaneous measurement of the level of expression of tens of thousands of genes in a given sample [9,10]. With this approach, it is thus possible to obtain a total gene expression profile or 'transcriptome' for each of the various stages of MDS and then to compare these profiles either among MDS stages or with those of the healthy condition, AA or *de novo* AML. Such analysis has the potential both to identify novel molecular markers for the differential diagnosis of MDS vs AA or *de novo* AML as well as to reveal genes that contribute to the pathogenesis of MDS. It might also be possible to determine whether MDS should be treated as a clinical entity distinct from AA or *de novo* AML.

It is important to bear in mind, however, that blood cells of different lineages and differentiation levels possess markedly different transcriptomes, even within the same individual. Any shift in cell composition in the specimens analysed will, thus, greatly influence the gene expression profile determined by micro-array studies [11].

Normal vs MDS

Several studies have attempted to compare transcriptomes between healthy individuals and patients with MDS in order to identify differences in gene expression. Pellagatti et al. [12] isolated RNA from differentiated granulocytes of 7 healthy individuals and 21 patients with MDS (17 with RA, 2 with RARS and 2 with RAEB according to the French-American-British (FAB) classification). The RNA was subjected to hybridization with a cDNA micro-array harboring probes corresponding to ~6000 human genes and the researchers identified 12 genes whose expression was frequently up-regulated (ratio of >2.0 in $\geqslant 9$ patients) or down-regulated (ratio of <0.5 in $\geqslant 10$ patients) in MDS. The relevance of these genes to the molecular diagnosis of MDS is unknown.

In contrast, Hofmann et al. [13] isolated $CD34^+$ progenitor fractions from the bone marrow of 4 healthy subjects and 11 MDS patients (7 low-risk and 4 high-risk according to the International Prognostic Scoring System [14]) for analysis with micro-arrays containing > 12 000 human probe sets. They identified 161 genes whose expression was down-regulated (ratio of <0.2) in low-risk MDS patients compared with healthy subjects. They also detected 117 genes whose expression was up-regulated (ratio of >5) in MDS patients and 27 of these genes encoded regulators of hematopoiesis, including acute myeloid leukemia 1 (AML1), activating transcriptional factor 3 (ATF3), homeobox 7 (HOX7) and Delta-like homolog 1 (DLK1).

Chen et al. [15] also chose $CD34^+$ cells for comparison of transcriptomes between healthy controls and MDS patients, specifically those with monosomy 7 or trisomy 8. $CD34^+$ progenitor cells were purified from the bone marrow of 4 control subjects, 4 MDS patients with trisomy 8 and 2 MDS patients with monosomy 7 and RNA isolated from these cells was subjected to hybridization with the same type of arrays (Affymetrix GeneChip HGU95Av2) as those used by Hofmann et al. [13]. Comparison of gene expression profiles among the subjects revealed that genes important in immune function and inflammation were frequently over-expressed in the MDS patients

with trisomy 8, consistent with previous findings implicating autoimmune activity in such patients [16]. In contrast, genes important in cell growth were often down-regulated in the patients with monosomy 7. These findings, thus, suggested that gene expression profiles differ between MDS blasts with trisomy 8 and those with monosomy 7.

Stage progression in MDS

A substantial proportion of MDS patients in early stages of the disease, especially those with an unfavorable karyotype [17], undergoes progression to advanced stages or to AML. Given that currently available chemotherapeutic regimens for advanced MDS are of limited efficacy, it would be clinically advantageous to block stage progression in MDS. Alterations of several oncogenes and tumor suppressor genes have been implicated in the progression of MDS [18]. Activating mutations of *RAS* genes are thought to be the most prevalent (affecting 10 – 30% of cases) of such changes in MDS [19,20]. It remains unclear, however, whether *RAS* mutation occurs at the early or late stages of MDS. Inactivation of the p53 gene is also apparent in 5 – 10% of MDS patients [21]. Again, however, it is not known whether loss of p53 function is an early or late event during MDS progression. In addition, epigenetic silencing of the p15 gene and shortening of telomeres have been detected in bone marrow cells of MDS patients [22]. None of these gene alterations is specific to MDS and it is unclear which changes are the cause of MDS itself and which are associated with stage progression.

To obtain insight into the mechanism of stage progression of MDS, in their comparison of gene expression profiles among healthy controls, low-risk MDS patients and high-risk MDS patients, Hofmann et al. [13] applied the class membership prediction method to identify genes whose expression was linked to separation of the 3 classes. They identified 11 such genes (Table I) and a simple 2-way clustering analysis of the study subjects based on the expression patterns of these 11 genes clearly separated the 3 major classes. Furthermore, a similar clustering analysis of a second set of subjects ($n = 8$) also separated individuals with high-risk MDS from those with low-risk MDS. Although the number of study subjects was small, these data support the notion that each stage of MDS has a characteristic gene expression profile or 'molecular signature'.

Table I. Genes used for class separation of healthy individuals and low- or high-risk patients with MDS [13].

Gene symbol	Accession number	Chromosomal position
TACSTD2	J04152	1p32
UQCRC1	L16842	3p21.3
TNNC1	M37984	3p21.3
KDELR	M88458	7p
CLC	L01664	19q13.1
H-PKL	M5422	7
RGS19	Z91809	
ATF3	L19871	1
FARP1	AI701049	
GNG7	AW051450	
TPD52L2	U44429	6q22-q23

CD133 (also known as AC133) is a cell surface protein that is expressed exclusively on $CD34^+$ $CD38^-$ hematopoietic stem cells (HSCs) [23,24]. Many AML blasts also express CD133 [25], indicating that the differentiation of these cells is blocked at a highly immature stage. The existence of 'cancer stem cells' for AML and solid tumors has been recently demonstrated and such cells express CD133 in brain tumors [26], as do $CD34^+CD38^-$ cells in AML [27]. Analysis of $CD133^+$ HSC-like fractions among MDS patients may, thus, reveal the character of 'MDS stem cells'. Analysis of such fractions also has the advantage of eliminating from micro-array data the influence of variation in cell composition of bone marrow, which is especially important given that different stages of MDS are characterized by different numbers of immature blasts within marrow.

Ueda et al. [28] performed micro-array analysis with $CD133^+$ cells isolated from the bone marrow of 2 healthy individuals, 11 patients with RA, 5 patients with RAEB and 14 patients with MDS-associated AML. Comparison of the gene expression profiles among the different stages of MDS led to the identification of 11 late stage (RAEB, MDS-associated AML)-specific genes and 6 early stage (healthy controls, RA)-specific genes. The latter set of genes included that for PIASy, which catalyses sumoylation of substrate proteins [29]. Loss of expression of the PIASy gene in advanced MDS suggested that the encoded protein might possess anti-tumor activity. Consistent with this notion, forced expression of PIASy in a mouse myeloid cell line resulted in rapid induction of apoptosis when the cells were cultured in the presence of granulocyte colony-stimulating factor (G-CSF) (Figure 2) [28]. These results suggest that PIASy functions to restrain cell growth and that loss of its expression may facilitate stage progression in MDS. Loss of PIASy expression has also been implicated in stage progression of chronic myeloid leukemia [30].

MDS-derived AML vs *de novo* AML

Although dysplastic morphology of blood cells is a hallmark of MDS and MDS-derived AML, such

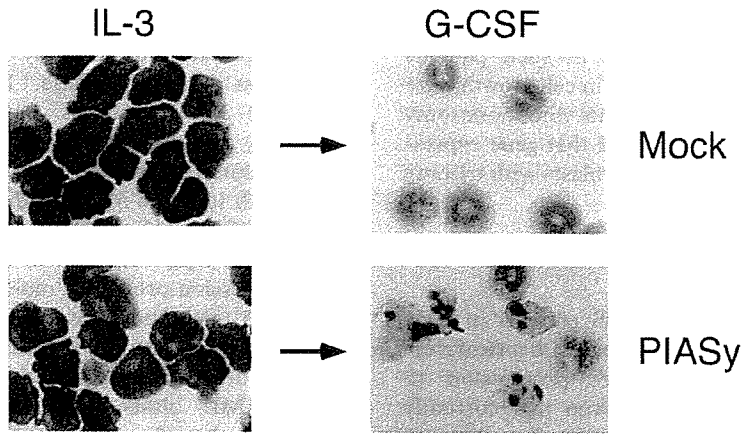

Figure 2. Induction of apoptosis by PIASy. 32Dcl3 cells were infected with a control retrovirus (Mock) or with a virus that encodes human PIASy and were then either maintained in the presence of interleukin-3 (IL-3) or exposed to G-CSF. Whereas control cells incubated with G-CSF underwent gradual differentiation into granulocyte-like cells, those expressing PIASy died rapidly by apoptosis on exposure to G-CSF. Reproduced with permission from Ueda et al. [28].

dysplasia is also apparent in the blood cells of some healthy older individuals. It is, thus, sometimes difficult to differentiate *de novo* AML from MDS-derived AML in the elderly, especially in the absence of a clinical history of the patient. Further complicating the issue, some younger patients with *de novo* AML also manifest blood cell dysplasia [31,32].

To provide insight into the differences or similarities between these clinical classes, Oshima et al. purified $CD133^+$ cells from the bone marrow both of 10 patients with *de novo* AML of the M2 sub-type, according to the FAB classification [33] and of 10 patients with MDS-derived AML corresponding to the M2 sub-type [34]. They then subjected RNA from these cells to micro-array analysis with HGU95Av2 micro-arrays. Comparison of samples matched for FAB sub-type was performed to minimize the influence of the differentiation ability of the blasts on gene expression profile; any differences in gene expression identified with this approach would, thus, be expected to be related with a high probability to the difference in the nature of MDS-derived AML from that of *de novo* AML.

Statistical analysis of the resulting expression data (Welch's ANOVA, $p < 0.01$; effect size of $\geqslant 5.0$ units) identified a total of 57 probe sets corresponding to genes whose expression was associated with diagnosis. However, a simple 2-way clustering analysis of the subjects based on the expression pattern for these probe sets failed to separate them into diagnosis-related sub-groups. To visualize the similarity or difference between the 2 classes, the researchers applied correspondence analysis, a method for the decomposition of multi-dimensional data [35]. This approach allows not only a low-dimensional projection of the expression profiles of numerous genes but also measurement both of the contribution of each gene to a given extracted dimension and of the contribution of each extracted dimension to the total complexity.

Correspondence analysis of the expression data for the 57 probe sets reduced the complexity from 57 to 3 dimensions. The specimens were then projected into a virtual space on the basis of their calculated 3-dimensional (3D) co-ordinates (Figure 3(*a*)). Most subjects with *de novo* AML were localized in a region of the space distinct from that occupied by those with MDS-derived AML. However, 2 individuals with *de novo* AML localized with those with MDS-derived AML. These observations indicated that the transcriptome of MDS-derived AML is distinct from that of *de novo* AML, but that current clinical diagnosis does not completely correlate with the difference in transcriptomes.

A similar analysis was performed on a larger scale by Tsutsumi et al. [36]. These researchers isolated $CD133^+$ cells from the bone marrow of patients with MDS-derived AML ($n = 11$), with *de novo* AML without dysplasia ($n = 15$), with *de novo* AML with multi-lineage dysplasia ($n = 11$) [32,37] or with therapy-related AML ($n = 2$). The study subjects were not limited to a specific FAB sub-type, however. The transcriptomes of these clinical classes were compared with the use of HGU95Av2 arrays. Comparison of *de novo* AML without dysplasia and MDS-derived AML led to the identification of 30 probe sets corresponding to genes whose expression was related to diagnosis. Correspondence analysis

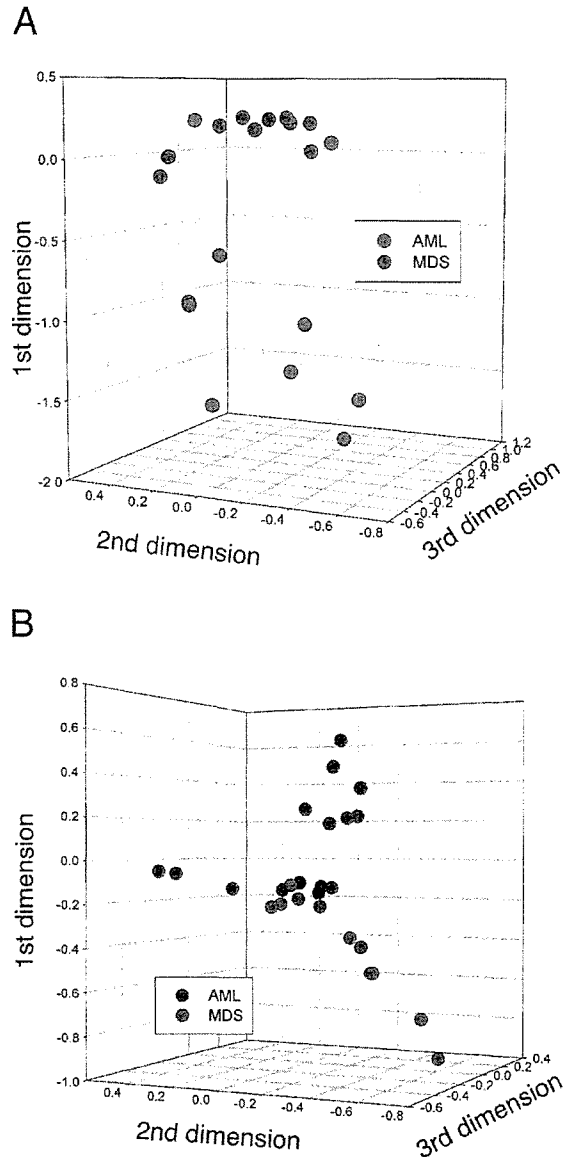

Figure 3. Analysis of the difference between the transcriptomes of MDS-related AML and *de novo* AML by 3D projection of study subjects. (*a*) Patients with *de novo* AML of the M2 sub-type (green) and those with MDS-derived AML of the M2 sub-type (red) were projected into a virtual space on the basis of co-ordinates calculated by correspondence analysis from the expression profiles of 57 probe sets shown in Oshima et al. [34]. (*b*) Patients with *de novo* AML without dysplasia (blue) and those with MDS-derived AML (red) were projected as in (*a*) on the basis of co-ordinates calculated from the expression profiles of 30 probe sets. Modified with permission from Tsutsumi et al. [36].

and 3D projection confirmed the distinct, but partially overlapping, gene expression profiles for the individuals diagnosed clinically with MDS-derived AML and those diagnosed with *de novo* AML without dysplasia (Figure 3(*b*)).

Future directions

DNA micro-array analysis has provided new insight into MDS. Such analysis allows comparison of transcriptomes between the healthy condition and MDS, among the distinct stages of MDS and between MDS-derived AML and other types of AML. The results of such studies are likely to lead to the development of accurate means of differential diagnosis as well as to the identification of genes that are important determinants of the various characteristics of MDS. DNA micro-array analysis and other genomics approaches also may clarify whether MDS is a single clinical entity as well as its relations to other clonal disorder of HSCs.

As of now, however, our knowledge of MDS provided by DNA micro-array analysis is relatively limited and based on preliminary data. Studies with much larger numbers of subjects than those performed to date are required. It remains to be determined both how many sub-groups of MDS can be defined on the basis of gene expression profiles and how these sub-groups are related to clinical characteristics, especially to long-term prognosis of patients and to the chemosensitivity of blasts. Given that the bone marrow of individuals at distinct stages of MDS contains different proportions of immature blasts, fractionation of bone marrow (for isolation of $CD34^+$ or $CD133^+$ cells, for example) before micro-array analysis is desirable. The combination of DNA micro-array analysis and other genomics tools should then shed new light on this enigmatic and intractable disorder.

References

1. Heaney ML, Golde DW. Myelodysplasia. New England Journal of Medicine 1999;340:1649–1660.
2. Aul C, Giagounidis A, Germing U. Epidemiological features of myelodysplastic syndromes: results from regional cancer surveys and hospital-based statistics. International Journal of Hematology 2001;73:405–410.
3. Boultwood J, Wainscoat JS. Clonality in the myelodysplastic syndromes. International Journal of Hematology 2001;73: 411–415.
4. Harris NL, Jaffe ES, Diebold J, Flandrin G, Muller-Hermelink HK, Vardiman J, et al. World Health Organization classification of neoplastic diseases of the hematopoietic and lymphoid tissues: report of the Clinical Advisory Committee meeting—Airlie House, Virginia, November 1997. Journal of Clinical Oncology 1999;17: 3835–3849.
5. Molldrem JJ, Leifer E, Bahceci E, Saunthararajah Y, Rivera M, Dunbar C, et al. Antithymocyte globulin for treatment of the bone marrow failure associated with myelodysplastic syndromes. Annals of Internal Medicine 2002;137: 156–163.
6. International Human Genome Sequencing Consortium. Finishing the euchromatic sequence of the human genome. Nature 2004;431:931–945.

7. The C. elegans Sequencing Consortium. Genome sequence of the nematode *C. elegans*: a platform for investigating biology. Science 1998;282:2012–2018.
8. Adams MD, Celniker SE, Holt RA, Evans CA, Gocayne JD, Amanatides PG, et al. The genome sequence of *Drosophila melanogaster*. Science 2000;287:2185–2195.
9. Duggan DJ, Bittner M, Chen Y, Meltzer P, Trent JM. Expression profiling using cDNA microarrays. Natural Genetics 1999;21:10–14.
10. Cheung VG, Morley M, Aguilar F, Massimi A, Kucherlapati R, Childs G. Making and reading microarrays. Natural Genetics 1999;21:15–19.
11. Miyazato A, Ueno S, Ohmine K, Ueda M, Yoshida K, Yamashita Y, et al. Identification of myelodysplastic syndrome-specific genes by DNA microarray analysis with purified hematopoietic stem cell fraction. Blood 2001;98: 422–427.
12. Pellagatti A, Esoof N, Watkins F, Langford CF, Vetrie D, Campbell LJ, et al. Gene expression profiling in the myelodysplastic syndromes using cDNA microarray technology. British Journal of Haematology 2004;125:576–583.
13. Hofmann WK, de Vos S, Komor M, Hoelzer D, Wachsman W, Koeffler HP. Characterization of gene expression of $CD34^+$ cells from normal and myelodysplastic bone marrow. Blood 2002;100:3553–3560.
14. Greenberg P, Cox C, LeBeau MM, Fenaux P, Morel P, Sanz G, et al. International scoring system for evaluating prognosis in myelodysplastic syndromes. Blood 1997;89: 2079–2088.
15. Chen G, Zeng W, Miyazato A, Billings E, Maciejewski JP, Kajigaya S, et al. Distinctive gene expression profiles of CD34 cells from patients with myelodysplastic syndrome characterized by specific chromosomal abnormalities. Blood 2004;104: 4210–4218.
16. Sloand EM, Kim S, Fuhrer M, Risitano AM, Nakamura R, Maciejewski JP, et al. Fas-mediated apoptosis is important in regulating cell replication and death in trisomy 8 hematopoietic cells but not in cells with other cytogenetic abnormalities. Blood 2002;100:4427–4432.
17. Nösslinger T, Reisner R, Koller E, Gruner H, Tuchler H, Nowotny H, et al. Myelodysplastic syndromes, from French-American-British to World Health Organization: comparison of classifications on 431 unselected patients from a single institution. Blood 2001;98:2935–2941.
18. Fenaux P. Chromosome and molecular abnormalities in myelodysplastic syndromes. International Journal of Hematology 2001;73:429–437.
19. Mano H, Ishikawa F, Hirai H, Takaku F. Mutations of N-ras oncogene in myelodysplastic syndromes and leukemias detected by polymerase chain reaction. Japanese Journal of Cancer Research 1989;80:102–106.
20. Paquette RL, Landaw EM, Pierre RV, Kahan J, Lubbert M, Lazcano O, et al. N-ras mutations are associated with poor prognosis and increased risk of leukemia in myelodysplastic syndrome. Blood 1993;82:590–599.
21. Jonveaux P, Fenaux P, Quiquandon I, Pignon JM, Lai JL, Loucheux-Lefebvre MH, et al. Mutations in the p53 gene in myelodysplastic syndromes. Oncogene 1991;6:2243–2247.
22. Tien HF, Tang JH, Tsay W, Liu MC, Lee FY, Wang CH, et al. Methylation of the p15(INK4B) gene in myelodysplastic syndrome: it can be detected early at diagnosis or during disease progression and is highly associated with leukaemic transformation. British Journal of Haematology 2001;112: 148–154.
23. Hin AH, Miraglia S, Zanjani ED, Almeida-Porada G, Ogawa M, Leary AG, et al. AC133, a novel marker for human hematopoietic stem and progenitor cells. Blood 1997; 90:5002–5012.
24. Kratz-Albers K, Zuhlsdorp M, Leo R, Berdel WL, Buchner T, Serve H. Expression of AC133, a novel stem cell marker, on human leukemic blasts lacking CD34-antigen and on a human $CD34^+$ leukemic line: MUTZ-2. Blood 1998;92: 4485–4487.
25. Bühring H-J, Seiffert M, Marxer A, Weiß B, Faul C, Kanz L, Brugger W. AC133 antigen expression is not restricted to acute myeloid leukemia blasts but is also found on acute lymphoid leukemia blasts and on a subset of $CD34^+$ B-cell progenitor. Blood 1999;94:832–833.
26. Singh SK, Hawkins C, Clarke ID, Squire JA, Bayani J, Hide T, et al. Identification of human brain tumour initiating cells. Nature 2004;432:396–401.
27. Bonnet D, Dick JE. Human acute myeloid leukemia is organized as a hierarchy that originates from a primitive hematopoietic cell. Natural Medicine 1997;3:730–737.
28. Ueda M, Ota J, Yamashita Y, Choi YL, Ohki R, Wada T, et al. DNA microarray analysis of stage progression mechanism in myelodysplastic syndrome. British Journal of Haematology 2003;123:288–296.
29. Sachdev S, Bruhn L, Sieber H, Pichler A, Melchior F, Grosschedl R. PIASy, a nuclear matrix-associated SUMO E3 ligase, represses LEF1 activity by sequestration into nuclear bodies. Genes Development 2001;15:3088–3103.
30. Ohmine K, Ota J, Ueda M, Ueno S-I, Yoshida K, Yamashita Y, et al. Characterization of stage progression in chronic myeloid leukemia by DNA microarray with purified hematopoietic stem cells. Oncogene 2001;20:8249–8257.
31. Brito-Babapulle F, Catovsky D, Galton DAG. Clinical and laboratory features of *de novo* acute myeloid leukemia with trilineage myelodysplasia. British Journal of Haematology 1987;66:445–450.
32. Taguchi J, Miyazaki Y, Yoshida S, Fukushima T, Moriuchi Y, Jinnai I, et al. Allogeneic bone marrow transplantation improves the outcome of de novo AML with trilineage dysplasia (AML-TLD). Leukemia 2000;14:1861–1866.
33. Bennett JM, Catovsky D, Daniel MT, Flandrin G, Galton DA, Gralnick HR, Sultan C. Proposed revised criteria for the classification of acute myeloid leukemia. A report of the French-American-British Cooperative Group. Annals of Internal Medicine 1985;103:620–625.
34. Oshima Y, Ueda M, Yamashita Y, Choi YL, Ota J, Ueno S, et al. DNA microarray analysis of hematopoietic stem cell-like fractions from individuals with the M2 subtype of acute myeloid leukemia. Leukemia 2003;17:1990–1997.
35. Fellenberg K, Hauser NC, Brors B, Neutzner A, Hoheisel JD, Vingron M. Correspondence analysis applied to microarray data. Proceedings of the National Academy of Sciences (USA) 2001;98:10781–1076.
36. Tsutsumi C, Ueda M, Miyazaki Y, Yamashita Y, Choi YL, Ota J, et al. DNA microarray analysis of dysplastic morphology associated with acute myeloid leukemia. Experimental Hematology 2004;32:828–835.
37. Kuriyama K, Tomonaga M, Matsuo T, Kobayashi T, Miwa H, Shirakawa S, et al. Poor response to intensive chemotherapy in *de novo* acute myeloid leukaemia with trilineage myelodysplasia. Japan Adult Leukaemia Study Group (JALSG). British Journal of Haematology 1994;86:767–773.

International Journal of
HEMATOLOGY

Clonally Expanded T-Cells in the Peripheral Blood of Patients with Idiopathic Thrombocytopenic Purpura and *Helicobacter pylori* Infection

Midori Ishiyama,[a] Masanao Teramura,[a] Koji Iwabe,[a] Tomohiro Kato,[b] Toshiko Motoji[a]

[a]Department of Haematology, Tokyo Women's Medical University, Tokyo; [b]Rheumatology, Immunology and Genetics Program, Institute of Medical Science, St. Marianna University School of Medicine, Kanagawa, Japan

Received August 1, 2005; received in revised form November 2, 2005; accepted November 14, 2005

Abstract

Eradication of *Helicobacter pylori* leads to platelet recovery in some patients with idiopathic thrombocytopenic purpura (ITP). Therefore, the pathogenesis of a subgroup of ITP is probably associated with *H pylori* infection (*H pylori*–related ITP). If *H pylori*–related ITP is a definite subgroup of ITP, specific oligoclonal T-cells might accumulate in the peripheral blood (PB). To address this issue, we performed single-strand conformation polymorphism analysis of complementarity-determining region 3 (CDR3) of the T-cell receptor β-chain genes of PB T-cells. Fourteen ITP patients with *H pylori* infection and 12 age-adjusted healthy volunteers were studied. Of the 14 patients, 8 patients (responders) exhibited a platelet response after successful *H pylori* eradication therapy, but 6 patients (nonresponders) did not. Vβ5.2, Vβ15, and Vβ19 gene usage by clonally expanded T-cells in PB obtained before *H pylori* eradication therapy was significantly higher in responders than in nonresponders or healthy volunteers (Vβ5.2, $P = .023$; Vβ15, $P = .004$; Vβ19, $P = .036$). Furthermore, an abrogation of clonally expanded T-cells was observed after therapy in some responders. These findings suggest that specific T-cell clones accumulate in *H pylori*–related ITP and that such clones may be associated with immune-mediated destruction of platelets.
Int J Hematol. 2006;83:147-151. doi: 10.1532/IJH97.05119

Key words: Idiopathic thrombocytopenic purpura (ITP); *Helicobacter pylori*; T-cell clonality; T-cell receptor; Single-strand conformation polymorphism (SSCP)

1. Introduction

Idiopathic thrombocytopenic purpura (ITP) is an autoimmune disorder caused by autoantibodies against platelets. Platelet membrane glycoproteins (GPs) such as GP IIb-IIIa and GP Ib have been identified as target autoantigens. Recently, many investigators reported that eradication of *Helicobacter pylori* leads to platelet recovery in patients with ITP (response rate, 33%-100%) [1-11]. However, a few investigators have shown the opposite result [12-14]. Therefore, *H pylori* infection may play an important pathophysiological role in a subgroup of ITP (*H pylori*–related ITP).

Oligoclonal T-cells that respond to antigenic stimulation accumulate in the peripheral blood (PB) in autoimmune diseases. Single-strand conformation polymorphism (SSCP) analysis of complementarity-determining region 3 (CDR3) of the T-cell receptor (TCR) β chain has demonstrated that oligoclonal T-cells accumulate in the PB of ITP patients [15]. This result suggests that specific oligoclonally expanded T-cells that drive B-cells to produce autoantibodies against platelets may be present in the PB of patients with ITP.

H pylori infection is prevalent among healthy people. In Japan, the frequency of *H pylori* infection is greater than 50% in healthy adults and 70% to 80% among elderly people [16]. Therefore, the occurrence of complicating *H pylori* infection in ITP patients does not necessarily mean that these patients have *H pylori*–related ITP. The diagnosis of *H pylori*–related ITP is made retrospectively according to the platelet response following *H pylori* eradication therapy. If a patient with *H pylori* infection recovers from thrombocytopenia after successful eradication therapy (ie, a responder), a diagnosis of *H pylori*–related ITP can be made. On the other hand, if a patient fails to recover from thrombocytopenia even after *H pylori* has successfully been eradicated (ie, a nonresponder), a diagnosis of *H pylori*–unrelated ITP can be made. If specific clonally expanded T-cells that are different from those of nonresponders and healthy volunteers can be demonstrated to be present in the PB of responders, it may

Correspondence and reprint requests: Masanao Teramura, MD, Department of Haematology, Tokyo Women's Medical University, 8-1, Kawada-cho, Shinjuku-ku, Tokyo, 162-8666, Japan; 81-3-3353-8111; fax: 81-3-5269-7363 (e-mail: teramura@dh.twmu.ac.jp).

Table 1.
Clinical and Laboratory Characteristics of 14 Patients with Idiopathic Thrombocytopenic Purpura*

Patient No.	Age, y	Sex	Disease Duration, mo	Previous Treatment	^{13}C-Urea Breath Test, ‰		*H pylori* Eradication	Platelets, $\times 10^9$/L		Response
					Before *H pylori* Eradication	After *H pylori* Eradication		Before *H pylori* Eradication	After *H pylori* Eradication	
1	50	M	38	PSL	38	0.9	Yes	14	138	+
2	52	M	6	—	16	2.1	Yes	14	239	+
3	56	M	18	PSL	4	1.3	Yes	54	95	+
4	56	M	10	PSL	14.9	1.8	Yes	18	105	+
5	63	F	23	PSL, Sp	10.2	1.2	Yes	20	92	+
6	74	F	58	Vitamin C	20	1.1	Yes	49	182	+
7	74	F	6	—	19.8	1.4	Yes	35	125	+
8	76	M	11	—	3	1.2	Yes	23	95	+
9	34	F	9	PSL	43.8	0.2	Yes	52	67	–
10	43	F	133	mPSL, Dan	4.3	1	Yes	19	11	–
11	50	F	78	—	49.3	0.6	Yes	73	66	–
12	53	F	16	—	10.3	1.2	Yes	70	92	–
13	58	F	60	PSL	20.1	1.3	Yes	31	18	–
14	61	F	63	Vitamin C	39	0.8	Yes	38	43	–

*Eight patients (nos. 1-8) showed a platelet response after *Helicobacter pylori* eradication therapy, and 6 patients (nos. 9-14) did not show a platelet response after eradication therapy. PSL indicates prednisolone; Sp, splenectomy; mPSL, methylprednisolone; Dan, danazol.

be possible to show that *H pylori*–related ITP is indeed a definite subgroup of ITP. To address this issue, we performed SSCP analysis of TCR Vβ-chain genes of PB T-cells in ITP patients with *H pylori* infection and investigated T-cell repertoire usage by the clonally expanded T-cells.

2. Materials and Methods

2.1. Patients

Fourteen patients with chronic ITP complicated by *H pylori* infection were studied. The patients comprised 5 men and 9 women with a median age of 56 years (range, 35-72 years). Chronic ITP was defined as thrombocytopenia (platelets $<100 \times 10^9$/L) lasting for at least 6 months, normal or increased numbers of megakaryocytes in the bone marrow, and absence of other apparent causes of thrombocytopenia. *H pylori* infection was diagnosed by a positive value of greater than 2.5% in the breath test using carbon 13 (^{13}C)-labeled urea [17].

H pylori infection was initially eradicated by treatment with amoxicillin (750 mg twice daily), clarithromycin (200 mg twice daily), and lansoprazole (30 mg twice daily) for 7 days. After a minimum of 2 months, the ^{13}C-urea breath test was again performed to evaluate the effect of *H pylori* eradication therapy. *H pylori* was eradicated in 12 of the 14 patients. The 2 patients (patients 13 and 14) who failed to respond were then successfully treated with metronidazole (250 mg twice daily), amoxicillin (750 mg twice daily), and lansoprazole (30 mg twice daily). Therefore, *H pylori* infection was eventually eradicated in all 14 patients.

The platelet response due to *H pylori* eradication was evaluated 6 months after treatment. A response was defined as an absolute increase in the platelet count of $>30 \times 10^9$/L from the baseline. The response criteria are based on the previous report by Vianelli et al [18]. As shown in Table 1, eradication of *H pylori* led to a platelet response in 8 patients (patients 1-8) but no response in 6 patients (patients 9-14). All of the responders are now in remission with a platelet count of $>100 \times 10^9$/L for at least 34 months after treatment.

2.2. SSCP Analysis of TCR β-Chain Genes

Samples of heparinized PB were obtained from all patients before eradication therapy. Samples were also obtained 3 to 6 months after eradication therapy for some patients. As a control, PB samples were also obtained from 12 age-adjusted healthy volunteers (5 men and 7 women with a median age of 57.5 years [range, 35-72 years]) with no history of recent infection. All patients gave informed consent.

SSCP analysis of TCR β-chain genes was performed as described elsewhere [19]. In brief, mononuclear cells were separated from the PB samples by density-gradient centrifugation over Ficoll-Paque (Amersham Biosciences, Uppsala, Sweden), and total RNA was extracted by the acid guanidinium thiocyanate–phenol–chloroform method [20]. RNA was converted to complementary DNA in a solution containing 200 U reverse transcriptase (SuperScript; Gibco BRL, Gaithersburg, MD, USA) and 100 pmol random hexamer oligonucleotide primer (Gibco BRL). For amplification of each TCR Vβ gene family, a biotinylated primer for the constant region of the β chain and a Vβ-specific primer were used. The sequences of the Vβ-specific primers were as described elsewhere [21]. The polymerase chain reaction was performed with deoxynucleoside triphosphates and *Taq* DNA polymerase (TaKaRa Bio, Shiga, Japan) for 35 cycles in a thermocycler (PerkinElmer, Norwalk, CT, USA). Following dilution and heat denaturation, amplified DNA fragments were separated on the basis of differences in their single-strand conformation by electrophoresis on nondenaturing 4% polyacrylamide gels containing 10% glycerol. The electrophoresed DNA fragments were transferred to membranes (GeneScreen; NEN Life Science Products, Boston, MA, USA) and visualized by subsequent incubations with strep-

tavidin, biotinylated alkaline phosphatase, and a chemiluminescent substrate system (Phototope-Star Detection kit; New England BioLabs, Beverly, MA, USA). We counted distinct bands as corresponding to clonal T-cell expansions. Although bands usually were easily recognized visually, a densitometer (ACD-25DX; ATTO Technology, Tokyo, Japan) was also used to confirm the presence of the bands. If one or more distinct bands were present in a certain Vβ gene family, the existence of clonally expanded T-cells was demonstrated. The presence of clonally expanded T-cells in each TCR Vβ gene family was individually assessed, and then the proportion of patients (or healthy volunteers) with clonally expanded T-cells was calculated for each TCR Vβ gene.

2.3. DNA Sequencing

TCR Vβ gene transcripts obtained before and after eradication therapy from one patient who had recovered from thrombocytopenia after *H pylori* eradication were extracted from the SSCP gel and cloned with a TA cloning kit (Invitrogen, Carlsbad, CA, USA). Approximately 20 plaques were randomly chosen and subjected to dideoxy direct sequencing.

2.4. Statistical Analysis

Differences in proportions among the groups were evaluated by the Kruskal-Wallis test, the Student *t* test, or the chi-square test. A P value <.05 was considered statistically significant.

3. Results

3.1. Analysis of the Clonally Expanded T-Cells in ITP Patients with H pylori Infection

We performed SSCP analyses of 20 major TCR Vβ gene families in patients with *H pylori* infection to investigate whether clonally expanded T-cells were present in PB. The median number of TCR Vβ gene families with clonally expanded T-cells in responders, nonresponders, and healthy subjects was 7 (range, 1-21), 3.5 (range, 2-11), and 4 (range, 1-6), respectively. The number of Vβ gene families with clonally expanded T-cells was significantly greater in responders (P = .032).

TCR Vβ subfamilies that frequently (>50% of cases) revealed clonally expanded T-cells were observed in 7 families (Vβ1, Vβ2, Vβ5.2, Vβ7, Vβ11, Vβ15, and Vβ19) in responders, 2 families (Vβ1 and Vβ5.1) in nonresponders, and 3 families (Vβ7, Vβ10, and Vβ11) in healthy volunteers (Figure 1). We analyzed the differences in Vβ usage of clonally expanded T-cells among responders, nonresponders, and healthy volunteers and found that the usage of Vβ5.2, Vβ15, and Vβ19 genes of clonally expanded T-cells was significantly higher in responders than in nonresponders or healthy volunteers (Vβ5.2, P = .023; Vβ15, P = .004; Vβ19, P = .036). We investigated whether the distinct bands in the SSCP analysis of Vβ5.2 (patients 1, 2, 3, and 6), Vβ15 (patients 3, 4, and 8), or Vβ19 (patients 3, 6, and 8) genes that were found in some responders before therapy disappeared after therapy. Disappearance of distinct bands from Vβ5.2, Vβ15, and Vβ19 genes was observed in none of 4 responders, 1 (patient 3) of 3 responders, and 1 (patient 3) of 3 responders, respectively (data not shown).

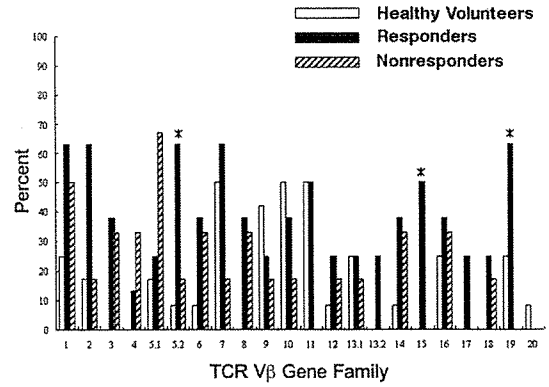

Figure 1. T-cell receptor (TCR) Vβ subfamily usage by clonally accumulated T-cells for responders, nonresponders, and healthy volunteers. Peripheral blood samples from patients with idiopathic thrombocytopenic purpura were obtained before eradication therapy and analyzed. If one or more distinct bands for a given Vβ gene were present in the single-strand conformation polymorphism analysis, the existence of clonally expanded T-cells was confirmed. The presence of clonally expanded T-cells for each TCR Vβ gene was individually assessed, and then the proportion of patients (or healthy volunteers) with clonal T-cell expansion was calculated for each TCR Vβ gene. Responders indicates patients who recovered from thrombocytopenia after successful *Helicobacter pylori* eradication; nonresponders, patients who failed to recover from thrombocytopenia even after *H pylori* was successfully eradicated. *Vβ5.2, Vβ15, and Vβ19 gene usage was significantly higher in responders than in nonresponders or healthy volunteers (P = .023, .004, and .036, respectively).

We compared nonresponders and healthy volunteers with respect to Vβ usage by clonally expanded T-cells and found Vβ3, Vβ4, Vβ5.1, and Vβ8 gene usage to be significantly higher in nonresponders (P = .034, .034, .034, and .034, respectively).

3.2. DNA Sequencing of TCR CDR3

In a patient (patient 1) who recovered from thrombocytopenia after *H pylori* eradication, the distinct band that was seen in the SSCP analysis of the Vβ8 gene before eradication therapy disappeared after eradication therapy (Figure 2). To confirm the disappearance of clonally expanded T-cells in Vβ8 following *H pylori* eradication, we determined the CDR3 DNA sequences of the TCR Vβ genes. In the sample obtained before *H pylori* eradication, all 18 subcloned genes showed the same sequence. However, in the sample obtained after *H pylori* eradication, all 19 subcloned genes showed different sequences, and none of these sequences were identical to the sequence seen before *H pylori* eradication (Table 2).

4. Discussion

We performed an SSCP analysis of TCR Vβ-chain genes of PB T-cells from ITP patients with *H pylori* infection and

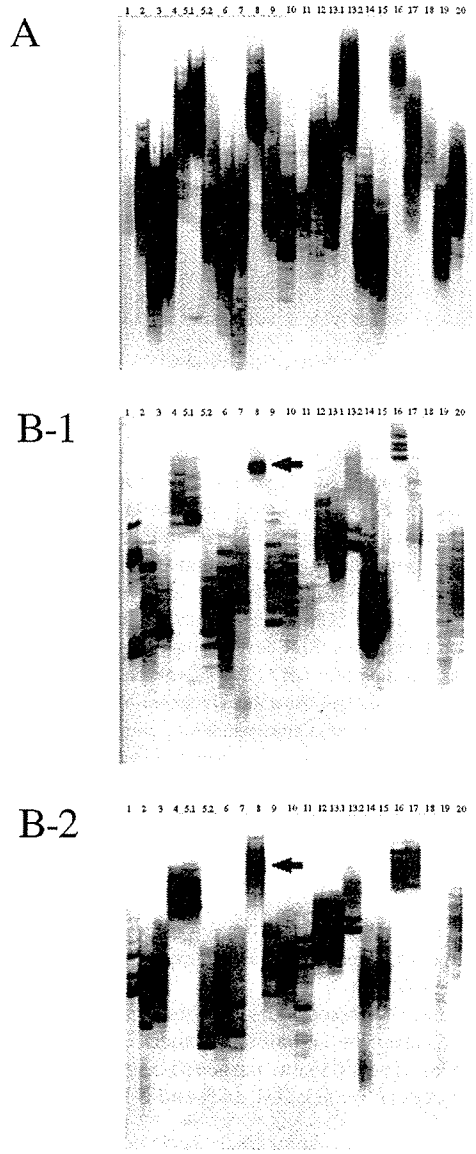

Figure 2. Single-strand conformation polymorphism analysis of T-cell receptor (TCR) Vβ genes in peripheral blood T-cells. The number at the top of each lane indicates the TCR Vβ gene subfamily. Results obtained from a typical healthy control subject (A) and patient 1 (responder) (B) are shown. In patient 1, a distinct band for the Vβ8 gene segment present before *Helicobacter pylori* eradication (B-1) disappeared after *H pylori* eradication (B-2) (arrows).

investigated T-cell repertoire usage by clonally expanded T-cells. The number of TCR Vβ gene families with clonally expanded T-cells was significantly higher in the patients with *H pylori* infection who subsequently recovered from thrombocytopenia after successful eradication therapy (responders) than in the patients who failed to recover from thrombocytopenia after successful eradication therapy (nonresponders). In addition, the usage of Vβ5.2, Vβ15, and

Table 2.
Deduced Amino Acid Sequences of the T-Cell Receptor (TCR) β Chains Carrying the Vβ Gene Segment Derived from the Peripheral Blood of Patient 1

Vβ8	nDn	Jβ (Gene Segment)	TCR β Chains, n
Before *Helicobacter pylori* eradication			
CASS	FSYCSA	NYGYT (J1S2)	18 (100%)
After *Helicobacter pylori* eradication			
CASSL	AWSGRY	TGELF (J2S2)	1 (5.3%)
CAS	RTTGG	SYEQY (J2S7)	1 (5.3%)
CASS	FSGGR	ETQYF (J2S5)	1 (5.3%)
CASS	KTGYE	QYFGP (J2S3)	1 (5.3%)
CAS	SRLAGGHPPT	QYFGP (J2S7)	1 (5.3%)
CAS	TRPEGGT	YNEQFF (J2S1)	1 (5.3%)
CAS	EEG	NTEAF (J1S1)	1 (5.3%)
CAS	SRFPAGA	YEQYF (J2S7)	1 (5.3%)
CA	SRPLAP	QETQYF (J2S5)	1 (5.3%)
CASS	SATV	SYEQY (J2S7)	1 (5.3%)
CASS	PRLDG	SYEQY (J2S7)	1 (5.3%)
CASS	RDFRA	NYGYT (J1S2)	1 (5.3%)
CASS	FGGTAR	QETQYF (J2S5)	1 (5.3%)
CASS	GTGTTSD	EQFFGPG (J2S1)	1 (5.3%)
CASSL	RPY	QPQHFG (J1S5)	1 (5.3%)
CAS	QGQH	NSPLHF (J1S6)	1 (5.3%)
CAS	NRLAGGHP	DTQYFGP (J2S3)	1 (5.3%)
CASSL	ELQDGYA	FGSGTRL (J1S2)	1 (5.3%)
CAS	RL	SGANVLT (J2S6)	1 (5.3%)

Vβ19 genes by clonally expanded T-cells was significantly higher in responders than in nonresponders. This difference notably does not derive from the presence or absence of *H pylori* infection, because all of the patients had been infected with *H pylori*. These results suggest that some clonally expanded T-cells with specific TCR Vβ subfamily usage are present in patients with *H pylori*–related ITP. Distinct bands seen in the SSCP analysis of Vβ genes before *H pylori* eradication therapy in some of the responders disappeared after *H pylori* eradication therapy. Furthermore, we confirmed the disappearance of clonally expanded T-cells after *H pylori* eradication therapy in a patient with *H pylori*–related ITP by analyzing the DNA sequences of CDR3 of Vβ genes. Our results indicate that clonally expanded T-cells were abrogated by *H pylori* eradication and suggest that the disappearance of clonally expanded T-cells was responsible for platelet recovery.

H pylori infection is associated with various autoimmune diseases, including rheumatoid arthritis, Sjögren syndrome, and autoimmune hypothyroidism [22-25]. Clinical data from patients with these disorders raise the possibility that immune reactions against *H pylori* have pivotal roles in the onset of autoimmune diseases. As for *H pylori*–related ITP, why *H pylori* eradication is able to induce platelet recovery is unknown. However, one possible explanation is that anti–*H pylori* antibodies bind to platelets in the presence of cross-mimicry between platelet surface antigens and *H pylori* antigens, resulting in platelet destruction. This speculation is supported by recent work demonstrating that platelet-associated immunoglobulin possesses cross-reactivity to

H pylori cytotoxin-associated gene A (CagA) [26]. If this mechanism operates in *H pylori*–related ITP, it strongly suggests that *H pylori* eradication induces a reduction in the T-cell clones against CagA that drive B-cells to produce cross-reactive antibodies, resulting in the reduction of cross-reactive antibodies. Our data demonstrating the subsequent disappearance of clonally expanded T-cells after *H pylori* eradication support this speculation.

Cytotoxic T-cell–mediated lysis of autologous platelets has recently been demonstrated in active ITP, and T-cell–mediated cytotoxicity has been suggested to be an alternative mechanism of platelet destruction in ITP [27]. Therefore, it is also possible that clonally expanded T-cells observed in *H pylori*–related ITP are cytotoxic T-cells against *H pylori* with cross-reactivity to platelets.

In conclusion, our findings suggest that specific T-cell clones accumulate in *H pylori*–related ITP and that these clones may be associated with immune-mediated platelet destruction. Further studies are needed to elucidate the role of the clonally expanded T-cells observed in *H pylori*–related ITP.

References

1. Gasbarrini A, Franceschi F, Tartaglione R, Landolfi R, Pola P, Gasbarrini G. Regression of autoimmune thrombocytopenia after eradication of *Helicobacter pylori*. *Lancet*. 1998;352:878.
2. Emilia G, Longo G, Luppi M, et al. *Helicobacter pylori* eradication can induce platelet recovery in idiopathic thrombocytopenic purpura. *Blood*. 2001;97:812-814.
3. Kohda K, Kuga T, Kogawa K, et al. Effect of *Helicobacter pylori* eradication on platelet recovery in Japanese patients with chronic idiopathic thrombocytopenic purpura and secondary autoimmune thrombocytopenic purpura. *Br J Haematol*. 2002;118:584-588.
4. Veneri D, Franchini M, Gottardi M, et al. Efficacy of *Helicobacter pylori* eradication in raising platelet count in adult patients with idiopathic thrombocytopenic purpura. *Haematologica*. 2002;87: 1177-1179.
5. Hino M, Yamane T, Park K, et al. Platelet recovery after eradication of *Helicobacter pylori* in patients with idiopathic thrombocytopenic purpura. *Ann Hematol*. 2003;82:30-32.
6. Hashino S, Mori A, Suzuki S, et al. Platelet recovery in patients with idiopathic thrombocytopenic purpura after eradication of *Helicobacter pylori*. *Int J Hematol*. 2003;77:188-191.
7. Ando T, Tsuzuki T, Mizuno T, et al. Characteristics of *Helicobacter pylori*-induced gastritis and the effect of *H. pylori* eradication in patients with chronic idiopathic thrombocytopenic purpura. *Helicobacter*. 2004;9:443-452.
8. Sato R, Murakami K, Watanabe K, et al. Effect of *Helicobacter pylori* eradication on platelet recovery in patients with chronic idiopathic thrombocytopenic purpura. *Arch Intern Med*. 2004;164: 1904-1907.
9. Fujimura K, Kuwana M, Kurata Y, et al. Is eradication therapy useful as the first line of treatment in *Helicobacter pylori*-positive idiopathic thrombocytopenic purpura? Analysis of 207 eradicated chronic ITP cases in Japan. *Int J Hematol*. 2005;81:162-168.
10. Inaba T, Mizuno M, Take S, et al. Eradication of *Helicobacter pylori* increases platelet count in patients with idiopathic thrombocytopenic purpura in Japan. *Eur J Clin Invest*. 2005;35:214-219.
11. Stasi R, Rossi Z, Stipa E, Amadori S, Newland AC, Provan D. *Helicobacter pylori* eradication in the management of patients with idiopathic thrombocytopenic purpura. *Am J Med*. 2005;118: 414-419.
12. Jarque I, Andrew R, Llopis I, et al. Absence of platelet response after eradication of *Helicobacter pylori* infection in patients with chronic idiopathic thrombocytopenic purpura. *Br J Haematol*. 2001;115:1002-1003.
13. Michel M, Khellaf M, Desforges L, et al. Autoimmune thrombocytopenic purpura and *Helicobacter pylori* infection. *Arch Intern Med*. 2002;162:1033-1036.
14. Michel M, Cooper N, Jean C, Frissora C, Bussel JB. Does *Helicobater pylori* initiate or perpetuate immune thrombocytopenic purpura? *Blood*. 2004;103:890-896.
15. Shimomura T, Fujimura K, Takafuta T, et al. Oligoclonal accumulation of T cells in peripheral blood from patients with idiopathic thrombocytopenic purpura. *Br J Haematol*. 1996;95:732-737.
16. Asaka M, Kimura T, Kudo M, et al. Relationship of *Helicobacter pylori* to serum pepsinogen in an asymptomatic Japanese population. *Gastroenterology*. 1992;102:760-766.
17. Ohara S, Kato M, Asaka M, Toyota T. Studies of ^{13}C-urea breath test for diagnosis of *Helicobacter pylori* infection in Japan. *J Gastroenterol*. 1998;33:6-13.
18. Vianelli N, Valdre L, Fiacchini M, et al. Long-term follow-up of idiopathic thrombocytopenic purpura in 310 patients. *Haematologica*. 2001;86:504-509.
19. Yamamoto K, Sakoda H, Nakajima T, et al. Accumulation of multiple T cell clonotypes in the synovial lesions of patients with rheumatoid arthritis revealed by a novel clonality analysis. *Int Immunol*. 1992;4:1219-1223.
20. Chomczynski P, Sacchi N. Single-step method of RNA isolation by acid guanidinium thiocyanate-phenol-chloroform extraction. *Anal Biochem*. 1987;162:156-159.
21. Choi YW, Kotzin B, Herron L, Callahan J, Marrack P, Kappler J. Interaction of *Staphylococcus aureus* toxin "superantigens" with human T cells. *Proc Natl Acad Sci U S A*. 1989;86:8941-8945.
22. Gasbarrini A, Franceschi F. Autoimmune disease and *Helicobacter pylori* infection. *Biomed Pharmacother*. 1999;53:223-226.
23. Zentilin P, Seriolo B, Dulbecco P, et al. Eradication of *Helicobacter pylori* may reduce disease severity in rheumatoid arthritis. *Aliment Pharmacol Ther*. 2002;16:1291-1299.
24. Figura N, Giordano N, Burroni D, et al. Sjögren's syndrome and *Helicobacter pylori* infection. *Eur J Gastroenterol Hepatol*. 1994;6: 321-322.
25. de Luis DA, Varela C, de La Calle H, et al. *Helicobacter pylori* infection is markedly increased in patients with autoimmune atrophic thyroiditis. *J Clin Gastroenterol*. 1998;26:259-263.
26. Takahashi T, Yujiri T, Shinohara K, et al. Molecular mimicry by *Helicobacter pylori* CagA protein may be involved in the pathogenesis of *H. pylori*-associated chronic idiopathic thrombocytopenic purpura. *Br J Haematol*. 2004;124:91-96.
27. Olsson B, Andersson PO, Jernas M, et al. T-cell-mediated cytotoxicity toward platelets in chronic idiopathic thrombocytopenic purpura. *Nat Med*. 2003;9:1123-1124.

Develop. Growth Differ. (2006) **48**, 177–188 doi: 10.1111/j.1440-169x.2006.00855.x

Peroxisome proliferator-activated receptor γ ligands stimulate myeloid differentiation and lipogenensis in human leukemia NB4 cells

Etsuko Yasugi,[1,*] Akiko Horiuchi,[3] Isao Uemura,[4] Emiko Okuma,[1] Masami Nakatsu,[1] Kumiko Saeki,[1] Yasushi Kamisaka,[6] Hiroyuki Kagechika,[5] Kazuki Yasuda[2] and Akira Yuo[1]

Departments of [1]Hematology and [2]Metabolic Disorder, Research Institute, International Medical Center of Japan, 1-21-1, Toyama, Shinjuku-ku, Tokyo 162-8655, [3]Division of Natural Sciences, International Christian University, 3-10-2, Osawa, Mitaka-shi, Tokyo 181-8585, [4]Department of Biological Science, Graduate School of Science, Tokyo Metropolitan University, 1-1, Minamiosawa, Hachioji, Tokyo 192-0397, [5]School of Biomedical Science, Tokyo Medical and Dental University, 2-3-10 Kanda-Surugadai, Chiyoda-ku, Tokyo 101-0062, and [6]Lipid Engineering Research Group, Research Institute of Biological Resources, National Institute of Advanced Industrial Science and Technology, Tsukuba, Ibaraki 305-8566, Japan

Peroxisome proliferator-activated receptor γ (PPARγ) plays a central role in adipocyte and macrophage differentiation. Pioglitazone (Actos, AD4833), an antidiabetic drug, and 15-deoxy-$\Delta^{12,14}$-prostaglandin J2 (PGJ2) have recently been identified as synthetic and natural ligands for PPARγ, respectively. In this study, we examined the effects of PPARγ ligands on differentiation and lipogenesis in promyelocytic leukemia NB4 cells, in which PPARγ protein was expressed and ligand-stimulated PPARγ-specific transcription of adipocyte fatty-acid binding protein was confirmed. Treatment with PPARγ ligand (AD4833 or PGJ2) alone markedly suppressed proliferation but did not induce differentiation. The combined treatment of the cells with PPARγ ligand and all-trans retinoic acid (ATRA) synergistically induced myelocytic differentiation, as determined by nitroblue tetrazolium reducing ability and cell morphology. During these processes of differentiation, we observed marked accumulation of lipid droplets in the cytoplasm. The cellular triacylglycerol levels increased 2.7-fold after treatment with the inducers. Simultaneously, BODIPY-fatty acid was incorporated into the cytosol and concentrated in lipid droplets. The biosynthesis of triacylglycerol-containing BODIPY-fatty acids was increased twofold in differentiated cells. These findings clearly demonstrate that treatment with PPARγ ligands not only induced differentiation but also stimulated lipogenesis in NB4 cells, indicating a close association between differentiation and lipogenesis in PPARγ-stimulated human myeloid cells.

Key words: differentiation, lipogenesis, NB4 cell, pioglitazone, PPARγ ligand.

Introduction

Peroxisome proliferator-activated receptor γ (PPARγ) is a member of the nuclear receptor superfamily and is a ligand-dependent transcription factor (Kliewer *et al.* 1992a; Kliewer *et al.* 1992b). This receptor functions as a central regulator in the process of adipocyte or macrophage differentiation as well as in lipid and glucose metabolism (Nagy *et al.* 1998; Tontonoz *et al.* 1998; Rosen *et al.* 1999). Its ligands include modified fatty acids, the prostaglandin D2 metabolite 15-deoxy-$\Delta^{12,14}$-prostaglandin J2 (PGJ2), and antidiabetic drugs such as thiazolidione, rosiglitazone or pioglitazone (Forman *et al.* 1995; Lehmann *et al.* 1995; Nagy *et al.* 1998). PPARγ binds to DNA as a heterodimer with the retinoid X receptor (RXR). This heterodimer is also activated by RXR ligands (Kliewer *et al.* 1992b; Gearing *et al.* 1993). Together, ligands specific for PPARγ and RXR can synergistically activate transcription and promote adipocyte differentiation in culture (Schulman *et al.* 1998; Thuillier *et al.* 1998).

In several myelocytic cell lines, such as HL-60, U937 and NB4, all-trans retinoic acid (ATRA), which binds to retinoic acid receptors (RAR), induces differentiation of these immature myeloid cells into mature phagocytic cells (Breitman *et al.* 1980; Hu *et al.* 1993). ATRA has

Etsuko Yasugi and Akiko Horiuchi contributed equally to this work.
*Author to whom all correspondence should be addressed.
Email: e-yasugi@umin.ac.jp
Received 5 December 2005; revised 18 January 2006; accepted 19 January 2006.

been used successfully for the treatment of patients with acute promyelocytic leukemia (APL; Huang *et al.* 1988; Degos 1992). However, this therapy has one problem, that is, the prolonged use of a high dose of ATRA provoked expression of cytosolic retinoic acid-binding proteins, which resulted in the leukemic cells becoming resistant to the induction of differentiation (Cornic *et al.* 1992). 9-*cis*-Retinoic acid (9-*cis* RA), an isomer of ATRA that can bind both RAR and RXR, also proved to be potent in inducing differentiation (Kizaki *et al.* 1993; Sakashita *et al.* 1993). In addition, Evans *et al.* reported that the combination of a PPARγ ligand and an RXRα ligand induced monocytic differentiation of some myeloid leukemia cell lines (HL-60 and THP-1) (Nagy *et al.* 1998; Tontonoz *et al.* 1998). Therefore, we considered that the combination of PPARγ ligands with retinoids, not only RXR ligands but also RAR ligands, might have synergetic effects on differentiation in the APL cell line NB4.

Peroxisome proliferator-activated receptor γ functions as a transcriptional regulator of genes related to lipid metabolism. Known targets of PPARγ include the genes encoding adipocyte fatty acid binding protein (aP2), phosphoenoylpyruvate carboxykinase, lipoprotein lipase, and the brown fat uncoupling protein UCP1 (Tontonoz *et al.* 1998). PPARγ is expressed at high levels in adipose tissues and serves as a central regulator of the process of adipocyte differentiation (Chawla *et al.* 1994; Tontonoz *et al.* 1994). This transcription factor may also play an important role in the regulation of lipid metabolism in other cell types, such as cells in mammary and colonic epithelia (Mueller *et al.* 1998) and monocyte/macrophages (Tontonoz *et al.* 1998). These facts led us to study the effects of PPARγ ligands in combination with a retinoid on lipogenesis in human myeloid NB4 cells.

In this study, we investigated the combined effects of ATRA (RAR ligand) and PPARγ ligands on human myeloid NB4 cells. Two major cell biological phenomena on which we focused were differentiation and lipogenesis, since RAR and PPARγ play important roles in both of these biological phenomena in human myeloid cells, and therefore we can explore possible linkage between them in our *in vitro* assay system. Our data showed that pioglitazone or PGJ2 in conjunction with ATRA inhibited clonal proliferation and potently induced the differentiation of NB4 cells to granulocytic maturation. Furthermore, cells exposed to the combination of PPARγ ligand and ATRA accumulated lipid droplets. The levels and biosynthesis of triacylglycerol in the cells increased markedly after differentiation. Taken together, these findings show that treatment with PPARγ ligand and ATRA exerted synergistic effects on differentiation and lipogenesis in NB4 cells.

Materials and methods

Chemicals

All-trans retinoic acid, PGJ2, and the synthetic PPARγ ligand pioglitazone (Actos, AD4833) were obtained from Sigma-Aldrich (St Louis, MO, USA), Cayman Chemical (Ann Arbor, MI, USA) and Takeda Chemical Industries, (Tokyo, Japan), respectively. These reagents were dissolved in ethanol. PPARγ antagonist (GW9662), RXR antagonist (HX531) and RXR agonists (LG100268, PA024) were synthesized (Boehm *et al.* 1995; Ebisawa *et al.* 1999; Ohta *et al.* 2000; Willson *et al.* 2001). PPARγ antagonist (BADGE) was obtained from Cayman Chemicals. All antagonists and agonists were dissolved in ethanol. Diluent alone had no effect on the proliferation or differentiation of leukemia cell lines. BODIPY FL dodecanoic acid (BODIPY-FL-C12), cholesteryl BODIPY FL C12 and nile red were from Molecular Probes (Eugene, OR, USA). Triacylglycerol-containing BODIPY-FL-C12 was synthesized from 1, 2-diacylglyceride (Funakoshi Co., Tokyo, Japan) and BODIPY-FL-C12 using Lipase D derived from Rhizopus delemar (Amano Pharmaceutical Co., Nagoya, Japan). Anti-PPARγ (H-100) antibody was obtained from Santa-Cruz Biotechnology (Santa Cruz, CA, USA).

Cell culture

Human myelocytic leukemia cell lines (NB4 and HL-60) were grown in RPMI-1640 medium (Sigma-Ardrich) with 10% fetal calf serum (FCS; JRH Biosciences, Lenexa, KS, USA) at 37°C in an atmosphere of 5% CO_2. Cell suspension (4×10^4 cells/mL) in RPMI-1640 medium containing 10% FCS was placed in each well of 6-well plates or 24-well plates. PPARγ ligand and ATRA were added to the culture medium. The cells were incubated for the indicated periods and harvested for experiments. To examine the effect of antagonists, the cells were pretreated with antagonist for 8 h prior to treatment.

Assessment of cell proliferation and differentiation

Cell growth after various treatments was assessed by counting viable cells under a phase contrast microscope (Olympus CK40; Olympus, Tokyo, Japan). Differentiation of leukemia cells was examined by assessing their ability to produce superoxide, as measured by reduction of nitroblue tetrazolium (NBT; Nacarai Tesque, Kyoto, Japan). For analysis of the ability to reduce NBT, samples of cultured cells were washed once and then suspended in RPMI-1640 medium supplemented with 10% FCS containing 1 mg/mL NBT and 100 ng/mL 12-O-tetradecanoylphorbol 13-acetate (Sigma) for 30 min at 37°C. Cells containing

formazan blue-black deposits were detected light microscopy (Olympus BX-51) and counted. To further confirm cell differentiation, cytocentrifuged preparations of cells were stained with Wright-Giemsa solution and observed under a light microscope.

Ultrastructural analysis

For morphological observation of differentiation and lipid droplets, electron microscopy was used. Methods of fixation, staining, embedding and sectioning were described previously (Yasugi *et al.* 2002). Sections were examined with an electron microscope (JEOL JEM1010; JEOL, Tokyo, Japan) and images were taken with the Imaging Plate system (PIX system 20; JEOL).

Preparation of cell lysates, gel electrophoresis and immunoblotting

Cell pellets were suspended in 1× sample buffer and mixed vigorously. The cell suspension was heated for 5 min at 100°C and then frozen at –20°C until use. Proteins were separated by electrophoresis in a 10% sodium dodecyl sulfate–polyacrylamide gel and transferred to a polyvinylidene difluoride membrane in blotting buffer. After transfer, the membrane was blocked with 5% non-fat dry milk in phosphate-buffered saline (PBS) for 1 h at room temperature. After incubation with primary antibody against PPARγ, horseradish peroxidase-conjugated secondary antibody followed by the enhanced chemiluminescence (ECL) system from Amersham Biosciences (Piscataway, NJ, USA) were used for detection.

RNA analysis

Total RNA was obtained from cells using an RNeasy mini kit (QIAGEN, Hilden, Germany). The first strand cDNA was synthesized from 1 μg of total RNA using the Super Script II Transcriptase (Invitrogen Japan, Tokyo, Japan). For the polymerase chain reaction (PCR) assay, 1 μL of cDNA was used in a total volume of 50 μL containing 1× reaction buffer, 0.2 mM dNTP, 20 pmol of each primer, and 0.25 U of Ex Taq polymerase (Takara Bio., Otsu, Japan). PCR was performed in a GeneAmp PCR system 9600 (Applied Biosystems, Foster City, CA, USA) with the following temperature profile: denaturation at 95°C, primer annealing at 55°C, and primer extension at 72°C, each for 30 s. After an initial denaturation (95°C, 5 min), the cycle was performed 30 times, followed by a final extension step for 7 min at 72°C. The primers used for aP2 (Genbank accession number J02874) were as follows: sense primer, 5′-TCCAGTGAAAACTTTGATGATTAT-3′; antisense primer, 5′-ACGCATTCCACCACCAGTTTA-3′); as described before (Zilberfarb *et al.* 2001). The expected size of the PCR product was 320 bp. PCR products were visualized on a 2% agarose gel by ethidium bromide staining.

Lipid droplet staining in cells

Cells were fixed with 1% paraformaldehyde in PBS for 30 min at room temperature and washed with PBS. For detection of lipid droplets, the cells were stained with nile red at a final concentration of 0.1 μg/mL for 30 min at room temperature, and examined with a fluorescence microscope (Olympus BX-51). The cell morphology in the same fluorescent image was observed under a light microscope with Nomarski differential interference contrast (DIC). The fluorescent and DIC images of cells were captured by Aquacosmos (version 2.01) from a digital camera C4742-95 (Hamamatsu Photonics, Hamamatsu, Japan).

Quantitation of triacylglycerol

Each sample of cells was harvested after 4 days of treatment with PPARγ ligand and ATRA, and sonicated in water. Lipids were extracted from the homogenate with methanol–chloroform–water (2:1:0.8, v/v). Extracted lipid was evaporated to dryness and dissolved in chloroform–methanol (2:1, v/v). Total lipid was applied to a high performance thin-layer chromatography (HPTLC) silica gel plate (Kieselgel 60; Merk & Co., Whitehouse Station, NJ, USA). For detection of neutral lipid, the plate was developed with a solvent mixture of hexane–ethylacetate (1:1, v/v) and was stained with Morstein reagent (10% sulfuric acid solution containing 0.1% cesium sulfate and 5% ammonium pentamolybdate). Levels of triacylglycerol in cells were quantified enzymatically using a Triglyceride *G*-test Wako kit (Wako Pure Chemical Industries, Osaka, Japan).

Metabolism of fluorescent fatty acid analogues in NB4 cells

After treatment with PPARγ ligand and ATRA for 3 days, cells in 96-well plates were incubated in RPMI medium containing BODIPY-FL-C12 (10 ng/mL) for 2 min at room temperature. After washing, cells were subsequently chased in RPMI medium at room temperature for various periods and examined using a fluorescence microscope. The intensity of incorporated BODIPY-FL-C12 fluorescence in the cells was analyzed using a FluorImager 595 (Amersham Biosciences).

For detection of triacylglycerol synthesis, cells were incubated with BODIPY-FL-C12 for 10 min at room temperature, washed and further incubated for

30 min at 37°C. Lipids extracted from the cells were separated on HPTLC plates with a solvent mixture of hexane–diethylether (1:1, v/v), visualized using a FluorImager 595, and quantified as percentage using Image Quant software.

Triacylglycerol synthesis was assayed *in vitro* in a final volume of 300 μL containing 16 μM BODIPY-FL-C12, 36 μM coenzyme A sodium salt, 0.5 M Tris-HCl buffer (pH 7.5) and cell homogenate (125 μg of protein) as an enzyme source. Glycerol and dihydroxyacetone phosphate lithium salt were used as substrates. Incubation was carried out for 30 min at room temperature and terminated by the addition of 2 mL of ethyl acetate. Lipids were extracted twice with ethyl acetate for 2 min by vigorously shaking. Then the combined organic phases were applied to HPTLC plates. Triacylglycerol containing BODIPY-FL-C12 was visualized with a FluorImager 595 and its amount was estimated as described above.

Protein determination

Protein content was measured using the BCA Protein Assay Reagent (Pierce, Rockford, IL, USA).

Statistical analysis

Statistical significance was determined by using Student's *t*-test (two-tailed) to compare the two groups of data sets. Asterisks shown in the figures and tables indicate significant differences between experimental conditions and the corresponding control condition.

Results

Presence of peroxisome proliferator-activated receptor γ protein and the growth-suppressive effect of peroxisome proliferator-activated receptor γ ligands in myeloid cells

Peroxisome proliferator-activated receptor γ protein in untreated and differentiated NB4 cells was detected by western blotting. The relative molecular mass of the PPARγ protein was 52 KDa. The expression of PPARγ protein was found in untreated cells. Treatment with PPARγ ligand alone or with a combination of PPARγ ligand and ATRA for 2 days (Fig. 1) or 4 days (data not shown) resulted in expression levels equivalent to those in untreated cells.

The effects of PPARγ ligand and ATRA on the proliferation of NB4 cells are shown in Table 1. PPARγ ligand (PGJ2 (4 μM) or AD4833 (50 μM)) alone caused a dramatic decrease of cell growth after 4 days of incubation, though ATRA (1 nM) had less effect. Combined treatment with ATRA plus PGJ2 or AD4833 caused a further decrease in the number of viable cells.

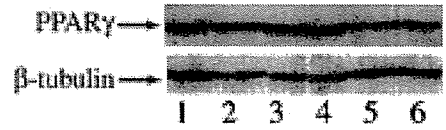

Fig. 1. Intracellular levels of peroxisome proliferator-activated receptor γ (PPARγ) protein in NB4 cells. Cells were treated with PPARγ ligand and/or all-trans retinoic acid (ATRA) for 2 days, and then whole cell extracts were subjected to western blot analysis. 1, Control; 2, 1 μM ATRA; 3, 4 μM 15-deoxy-Δ12,14-prostaglandin J2 (PGJ2); 4, 50 μM AD4833; 5, 1 μM ATRA + 4 μM PGJ2; 6, 1 μM ATRA + 50 μM AD4833.

Table 1. Effects of peroxisome proliferator-activated receptor γ ligands on NB4 cell growth

Treatment	Cell number (×10⁴)
Untreated	106.0 ± 4.3
1 nM ATRA	79.5 ± 3.5
4 μM PGJ2	34.7 ± 2.6
50 μM AD4833	47.0 ± 5.2
1 nμ ATRA + 4 μM PGJ2	26.7 ± 0.9
1 nM ATRA + 50 μM AD4833	31.7 ± 3.3

Cell number was counted after 4 days of treatment. Values are mean ± SD. ATRA, all-trans retinoic acid; PGJ2, 15-deoxy-Δ12,14-prostaglandin J2.

Peroxisome proliferator-activated receptor γ ligand and all-trans retinoic acid cooperate to promote NB4 differentiation

The differentiation of NB4 cells was evaluated by assessing the ability to reduce NBT, Wright-Giemsa staining and electron microscopic observation. With regard to NBT-reducing activity, neither PGJ2 nor AD4833 alone increased the activity of cells (data not shown). The combined treatment of cells with ATRA (1 nM) and PPARγ ligand strongly enhanced the NBT-reducing activity. More than 90% of cells treated with PPARγ ligand plus ATRA cells were positive for this activity, although ATRA-treated cells showed only 22% positivity (Fig. 2a). A high concentration of ATRA (1 μM) alone resulted in 96% of the cells being positive for NBT-reducing activity. In HL-60 cells, similar effects of PPARγ ligands and ATRA on differentiation were observed, although treatment with PGJ2 or AD4833 alone induced differentiation in these cells (Fig. 2b).

Next, the granulocytic differentiation of NB4 cells was morphologically confirmed by Wright-Giemsa staining (Fig. 3A). The cells treated with ATRA (1 nM) and PPARγ ligand showed lobulated kidney-bean or

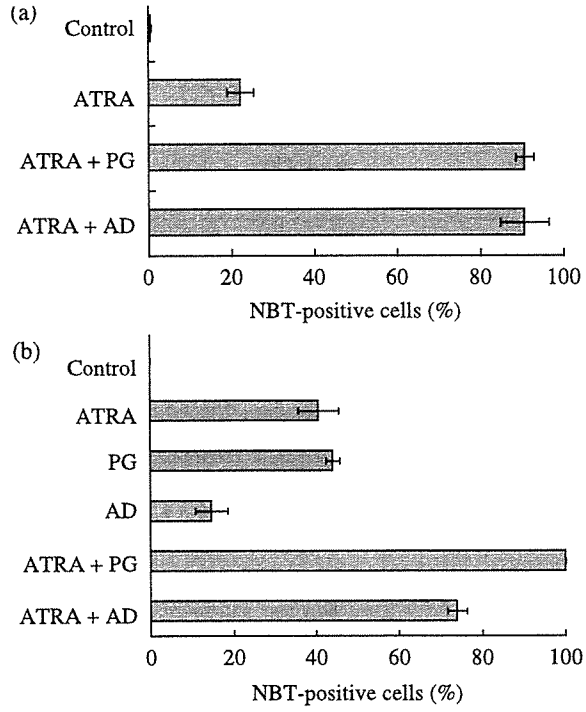

Fig. 2. Effects of peroxisome proliferator-activated receptor γ (PPARγ) ligands on nitroblue tetrazolium (NBT)-reducing activity in human myeloid cells. The NBT-reducing activities of NB4 (a) and HL-60 cells (b) were determined after 4 days of treatment with the indicated reagents. The activities are expressed as the percentage of NBT-positive cells. Results are representative of three experiments and are expressed as mean ± SD. (a) ATRA, 1 nM all-trans retinoic acid (ATRA); PG, 4 μM 15-deoxy-Δ12,14-prostaglandin J2 (PGJ2); AD, 50 μM AD4833. (b) ATRA, 1 μM ATRA; PG, 4 μM PGJ2; AD, 50 μM AD4833.

horse-shoe-shaped nuclei that are characteristic of granulocytes. The cytoplasm of those cells contained many white vacuoles and was stained white, in contrast to the blue cytoplasm of control cells. Furthermore ultrastructural observation showed that the combined treatment of cells with PPARγ ligand and ATRA (1 nM) induced irregularly lobulated nuclei and condensation of heterochromatin along the nuclear membrane (Fig. 3B). These results clearly indicate that PPARγ ligand and ATRA showed synergistic effects on granulocytic differentiation of NB4 cells.

Effects of peroxisome proliferator-activated receptor γ and retinoid X receptor antagonists on differentiation of NB4 cells

To confirm that the differentiation of NB4 cells is mediated through the PPARγ pathway, we used antagonists of PPARγ and RXR, such as GW9662 (Willson *et al.* 2001), BADGE (Wright *et al.* 2000) and HX531. HX531 works as an RXR antagonist (Ebisawa *et al.* 1999) but also as a potential PPARγ/RXR inhibitor (Yamauchi *et al.* 2001). The effects of PPARγ and RXR antagonists were evaluated in terms of the induced-differentiation of NB4 cells as determined by the NBT reduction assay. Their effects on ATRA ligand- and PPARγ ligand-induced NB4 differentiation are summarized in Table 2. All three antagonists showed inhibitory effects on the differentiation induced by the combination of ATRA and PPARγ ligands. In contrast, PPARγ antagonists did not exert an inhibitory effect on the differentiation of NB4 cells induced by ATRA

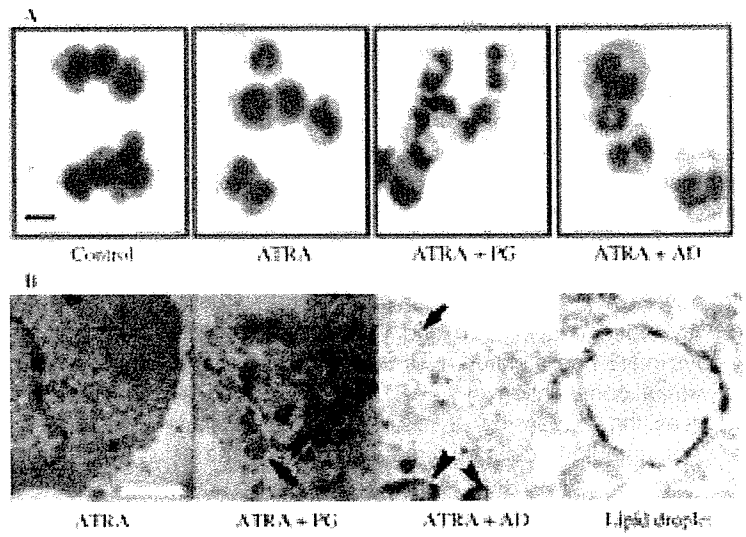

Fig. 3. Morphological observation of NB4 cells treated with peroxisome proliferator-activated receptor γ (PPARγ) ligand and/or all-trans retinoic acid (ATRA). The cells were treated for 4 days with ATRA (1 nM), PG (4 μM 15-deoxy-Δ12,14-prostaglandin J2), AD (50 μM AD4833), individually or combined. (A) Wright-Giemsa staining. Bar, 20 μm (B) Ultrastructural observation. Arrowhead and arrow indicate nucleus and lipid droplet, respectively. Bar, 4 μm. Right panel is higher magnification of the lipid droplet. Bar, 0.5 μm.

Table 2. Effects of peroxisome proliferator-activated receptor γ antagonists on NB4 differentiation

	None	HX531	GW9662	BADGE
1 μM ATRA	96.1 ± 2.2	95.0 ± 2.0	97.1 ± 0.2	94.3 ± 2.1
1 nM ATRA	22.0 ± 3.2	12.0 ± 2.2*	16.5 ± 8.8	25.5 ± 3.4
1 nM ATRA + 0.5 μM PGJ2	39.4 ± 4.9			28.7 ± 3.3*
1 nM ATRA + 2 μM PGJ2	91.7 ± 4.7	15.3 ± 1.0**	19.2 ± 3.8**	92.2 ± 2.1
1 nM ATRA + 50 μM AD4833	90.4 ± 5.8	3.2 ± 0.6***	5.6 ± 0.8***	26.3 ± 6.9**

Concentration of each antagonist was 1 μM. Values are expressed as percent of NBT-positive cells. Values are mean ± SD. Probabilities were calculated for the percentages of NBT-positive cells with and without peroxisome proliferator-activated receptor γ antagonist. *$P < 0.05$, **$P < 0.01$, ***$P < 0.001$. ATRA, all-trans retinoic acid; PGJ2, 15-deoxy-$\Delta^{12,14}$-prostaglandin J2.

Table 3. Effects of retinoic X receptor agonists on NB4 differentiation

	LG100268	PA024
None	0.8 ± 0.1	2.9 ± 0.7
4 μM PGJ2	74.8 ± 7.4***	26.3 ± 5.4**
50 μM AD4833	17.0 ± 1.3**	13.3 ± 3.5*

Concentration of each agonist was 1 μM. Values are expressed as percent of NBT-positive cells. Values are mean ± SD. Probabilities were calculated for the percentages of NBT-positive cells with and without peroxisome proliferator-activated receptor γ ligand. *$P < 0.05$, **$P < 0.01$, ***$P < 0.005$. PGJ2, 15-deoxy-$\Delta^{12,14}$-prostaglandin J2.

(1 nM or 1 μM) alone. Thus, for the induction of differentiation by the combination of ATRA and PPARγ ligands, the signaling through PPARγ/RXR is necessary. The combination of RXR agonist and PPARγ ligand also induced NB4 differentiation, indicating that the stimulation of the RXR receptor is important in this differentiation pathway (Table 3).

Upregulation of adipocyte fatty acid binding protein in NB4 cells during treatment with peroxisome proliferator-activated receptor γ ligands

The expression of adipocyte fatty acid binding protein (aP2), whose promoter has an adipose response element (ARE; DR-1), occurs in parallel to the expression of PPARγ (Thuillier *et al.* 1998). We examined the gene expression of aP2 in NB4 cells by reverse transcription–polymerase chain reaction (RT–PCR) after treatment with ATRA (1 μM) and PPARγ ligand (Fig. 4). The expression of aP2 mRNA was greatly induced after 24 h and continued for up to 4 days in NB4 cells cultured with PPARγ ligand alone or with a combination of PPARγ ligand and ATRA, whereas the expression of this gene remained low or undetectable in cells cultured with ATRA alone or in untreated cells. Thus, in human myeloid cells, PPARγ ligands induced the transcription of a gene specific for this transcriptional receptor and important for lipid metabolism.

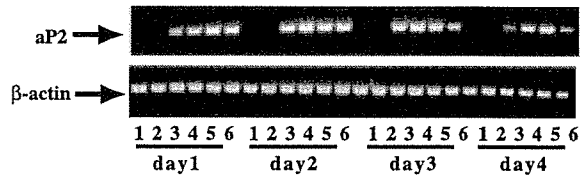

Fig. 4. Adipocyte fatty acid binding protein (aP2) mRNA expression in NB4 cells after treatment with peroxisome proliferator-activated receptor γ (PPARγ) ligand and/or all-trans retinoic acid (ATRA). Cells were treated with PPARγ ligand and/or ATRA for the indicated periods. Reverse transcription–polymerase chain reaction for aP2 mRNA in freshly prepared NB4 cells revealed a cDNA fragment of the expected size. 1, Control; 2, 1 μM ATRA; 3, 1 μM ATRA + 4 μM PGJ2; 4, 1 μM ATRA + 50 μM AD4833; 5, 4 μM PGJ2; 6, 50 μM AD4833. As a control for cDNA quality, the signals for β-actin expression are shown.

Lipid droplets accumulate in NB4 cells after treatment with peroxisome proliferator-activated receptor γ ligands and all-trans retinoic acid

In the cytoplasm of cells treated with PPARγ ligands and ATRA, we found many white vacuoles after Wright-Giemsa-staining, as mentioned above (Fig. 3A). We speculated that these vacuoles might be lipid droplets and examined the cells by fluorescence microscopy after staining with the lipophilic dye nile red. As nile red has the remarkable property of staining neutral lipids (Greenspan *et al.* 1985), lipid droplets containing triacylglycerol or cholesterol ester show a fluorescent red color. In Figure 5A, NB4 cells after treatment with PPARγ ligands and ATRA (1 μM) contained numerous nile red-positive droplets. In the cytoplasm of cells treated with ATRA alone, there were also lipid droplets, but the number of droplets was fewer and the intensity of the fluorescence was weaker. In the cells treated with PGJ2 or AD4833 alone, lipid droplets were weakly visible (data not

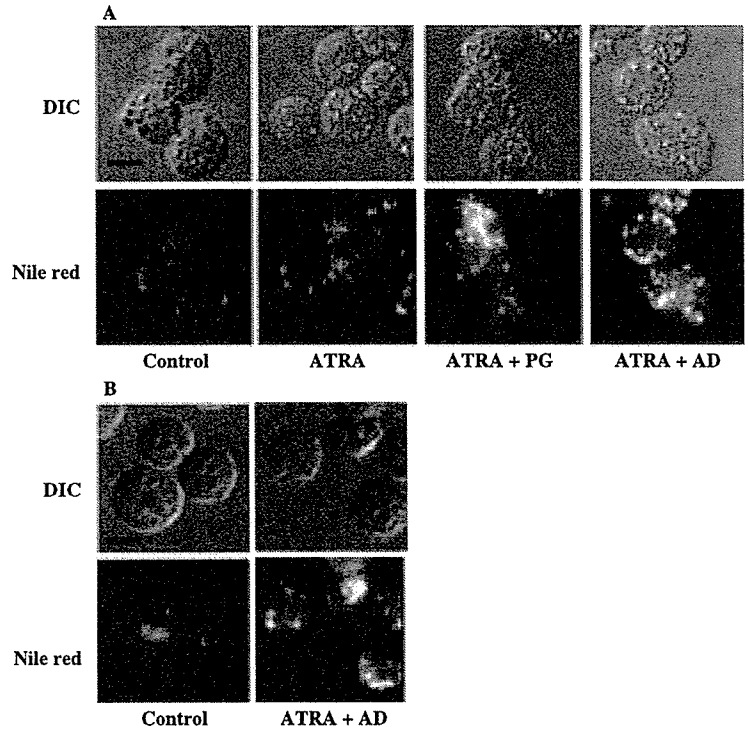

Fig. 5. Accumulation of lipid droplets in differentiated NB4 and HL-60 cells. Cells were treated for 4 days with all-trans retinoic acid (ATRA; 1 μM), ATRA (1 μM) + 15-deoxy-Δ12,14-prostaglandin J2 (PG; 4 μM) or ATRA (1 μM) + AD4833 (AD; 50 μM). Upper panels are difference interference contrast images, and lower panels are the corresponding images obtained by fluorescence microscopy. Lipid droplets were stained with nile red. Bar, 10 μm. (A) NB4 cells, (B) HL-60 cells.

shown). Similar findings were made in HL-60 cells (Fig. 5B). Ultrastructural observation revealed that treatment with PPARγ ligand and ATRA clearly stimulated the accumulation of lipid droplets in the cytoplasm (Fig. 3B). Lipid droplets are surrounded by a phospholipid monolayer, and clearly distinguished from other organelles in the cytoplasm. Both types of microscopic observation clearly demonstrated that PPARγ ligands stimulated the accumulation of lipid droplets in NB4 cells.

Triacylglycerol levels increase in NB4 cells after treatment with peroxisome proliferator-activated receptor γ ligands and all-trans retinoic acid

We examined whether treatment with PPARγ ligand and ATRA (1 μM) affected the cellular levels of triacylglycerol and cholesterol ester, the major storage lipids in mammalian cells. Thin-layer chromatography revealed that treatment with PPARγ ligand and ATRA particularly increased the triacylglycerol level in NB4 cells, and slightly increased the cholesterol ester level (Fig. 6a). Free-cholesterol levels were almost equivalent between untreated cells and cells treated with PPARγ ligand and ATRA. Next, the cellular triacylglycerol levels were analyzed enzymatically (Fig. 6b). After incubation with ATRA (1 μM) combined with PGJ2 or AD4833, the triacylglycerol level of NB4 cells was increased by 2.7-fold compared to that in untreated cells. PGJ2 or AD4833 alone also increased the triacylglycerol level slightly, but ATRA alone did not. These results strongly suggest that the lipid droplets in NB4 cells contained predominantly triacylglycerol, and the level of triacylglycerol increased after treatment of the cells with PPARγ ligand and ATRA.

Translocation of a fluorescent fatty acid analogue, BODIPY-FL-C12 in NB4 cells treated with peroxisome proliferator-activated receptor γ ligands and all-trans retinoic acid

The distribution pattern of intracellular BODIPY fluorescence was compared between differentiated and untreated cells under the pulse-chase conditions (Fig. 7a). After prelabeling of cells with BODIPY-FL-C12 at room temperature, intracellular fluorescence was distributed in the cytoplasm, including the endoplasmic reticulum (ER), in both differentiated and untreated cells. After a chase of 10–30 min, most of the intracellular fluorescence in differentiated cells was clearly accumulated in the lipid droplets, though that in untreated cells remained in the cytoplasm. The translocation of the fluorescence from the cytosol to lipid droplets was observed in differentiated cells treated with ATRA alone or with ATRA and PPARγ ligand. There was no significant difference in total

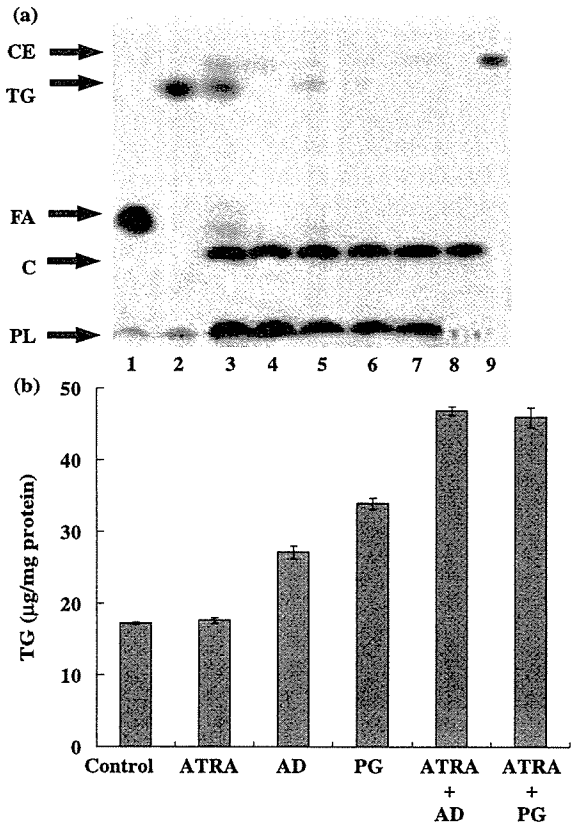

Fig. 6. (a) Thin-layer chromatogram of neutral lipids in differentiated NB4 cells. Each lane was spotted with crude lipid extracted from 7×10^4 cells. Cells were treated for 4 days with peroxisome proliferator-activated receptor γ (PPARγ) ligands and/or all-trans retinoic acid (ATRA). 1, linoleic acid; 2, trilinolein; 3, 1 μM ATRA + 4 μM 15-deoxy-Δ12,14-prostaglandin J2 (PGJ2); 4, control; 5, 1 μM ATRA + 50 μM AD4833; 6, 1 μM ATRA; 7, control; 8, cholesterol; 9, cholesterol ester. CE, cholesterol ester; TG, triacylglycerol; FA, fatty acid; C, cholesterol; PL, phospholipid. (b) Triacylglycerol levels in differentiated NB4 cells. Cells were treated for 4 days with PPARγ ligand and/or ATRA (1 μM). PG, 4 μM PGJ2; AD, 50 μM AD4833. Values represent mean ± SD. Triacylglycerol contents are expressed as μg/mg protein.

amount of BODIPY lipid associated with cells between the differentiated and untreated cells (data not shown). These observations provided evidence that BODIPY-FL-C12 was incorporated in the cytoplasm and immediately translocated to lipid droplets in differentiated cells.

Metabolism of BODIPY-FL-C12 in NB4 cells treated with peroxisome proliferator-activated receptor γ ligands and all-trans retinoic acid

In order to examine the metabolism of incorporated BODIPY-FL-C12, cells were prelabeled with BODIPY-FL-C12 at room temperature for 10 min and incubated for 30 min at 37°C. Extracted lipids containing BODIPY-FL-C12 were analyzed by thin-layer chromatography using a FluorImager. The fluorescent spots of triacylglycerol containing BODIPY-FL-C12 were detected in lipids extracted from both differentiated and untreated cells (data not shown). The Rf value of triacylglycerol containing BODIPY-FL-C12 was confirmed by the comigration of synthesized triacylglycerol containing BODIPY-FL-C12. The fluorescence of triacylglycerol extracted from cells treated with PPARγ ligands and ATRA was about twofold stronger than that of untreated cells (Fig. 7b). These findings indicated that BODIPY-FL-C12 had been incorporated in the cytoplasm and converted to triacylglycerol.

Triacylglycerol synthesis activity in differentiated and untreated cell homogenates was compared using two substrates, glycerol and dihydroxyacetone phosphate, respectively. The activity in differentiated cells treated with PPARγ ligands and ATRA was found to be more than twofold higher than that in untreated cells using glycerol as substrate (Fig. 7c). The activity was dependent on glycerol concentration (Fig. 7c) but not on dihydroxyacetone phosphate (data not shown).

These findings suggest that triacylglycerol was synthesized from glycerol in differentiated cells. Taken together, these data show that triacylglycerol synthesis in NB4 cells treated with PPARγ ligand and ATRA increased.

Discussion

Peroxisome proliferator-activated receptor γ has been demonstrated to regulate adipocyte differentiation and glucose homeostasis in response to several structurally distinct compounds, including thiazolidinediones (Tontonoz *et al.* 1994; Lehmann *et al.* 1995). In this study, we investigated the effects of PPARγ ligands on human NB4 and HL-60 cells and found that PPARγ ligands can act synergistically with ATRA to induce differentiation into cells that show granulocytic characteristics and accumulate lipid droplets. Activation of PPARγ in immortalized cell lines, such as THP-1 and HL-60, promotes differentiation along the macrophage lineage, as shown by changes in gene expression and uptake of OxLDL induced by CD36 (Hirase *et al.* 1999; Tontonoz *et al.* 1998). However, using PPARγ -deficient stem cells, Moore *et al.* demonstrated that PPARγ is neither essential for myeloid development nor for mature macrophage functions such as phagocytosis and inflammatory production (Moore *et al.* 2001). Furthermore, Asou *et al.* reported the effects of troglitazone on the proliferation and

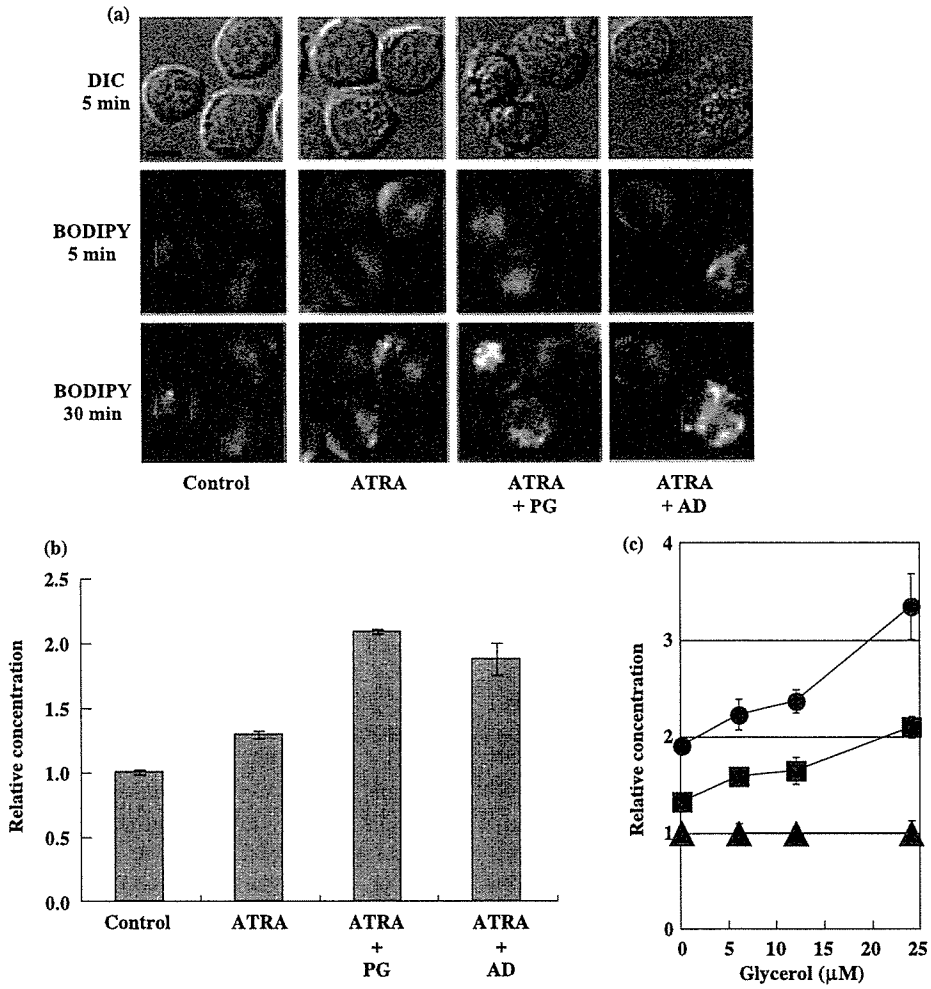

Fig. 7. (a) Intracellular distribution of BODIPY-FL-C12 fluorescence in differentiated and untreated NB4 cells. Cells were treated for 3 days with all-trans retinoic acid (ATRA; 1 μM), ATRA (1 μM) + 15-deoxy-Δ12,14-prostaglandin J2 (PG; 4 μM) or ATRA (1 μM) + AD (AD4833, 50 μM). Cells were incubated in medium containing BODIPY-FL-C12 for 2 min at room temperature and were subsequently chased and examined using a fluorescence microscope. Upper panels are difference interference contrast images. Middle and lower panels are the corresponding fluorescence microscopy images. BODIPY, BODIPY-FL-C12. Bar, 10 μm. (b) Relative concentration of triacylglycerol containing BODIPY-FL-C12 in NB4 cells. Cells were treated for 3 days with peroxisome proliferator-activated receptor γ (PPARγ) ligand (PGJ2 4 μM, AD4833 50 μM) and/or ATRA (1 μM). The assay methods are described in Materials and methods. Values represent mean ± SD. The relative concentrations of triacylglycerol containing BODIPY-FL-C12 in differentiated cells were calculated as fluorescence strength compared to that in untreated cells taken as 1.00. (c) Triacylglycerol synthesis activity in NB4 cells. Cells were treated for 3 days with PPARγ ligand (PGJ2 4 μM, AD4833 50 μM) and ATRA (1 μM). The method of the enzyme assay is described in Materials and methods. Values are mean ± SD. The relative concentrations of triacylglycerol containing BODIPY-FL-C12 in differentiated cells are plotted together with that of untreated cells taken as 1.00. (●), ATRA + PG; (■), ATRA + AD; (▲), control.

differentiation of normal and malignant myeloid cells (especially monocytic cells) and demonstrated that troglitazone combined with a retinoid was a moderately potent inhibitor of the clonogenic growth of acute myeloid leukemia cells, but not a potent inducer of differentiation of these leukemia cells (Asou *et al.* 1999). Our results clearly indicated that combined treatment with PPARγ ligand and ATRA induced differentiation of NB4 cells. This discrepancy between these findings may be related to the fact that in the study of Asou *et al.* (1999), NB4 cells were treated with troglitazone (10^{-5} M) as the PPARγ ligand, and the concentration of troglitazone was rather low compared to our conditions. We also examined the effects of PPARγ ligands and ATRA on HL-60 cells and observed synergistic effects of PPARγ ligands